

# Superplastic behavior of a fine-grained Mg–9Li material at low homologous temperature

Eric M. Taleff

*Department of Mechanical Engineering, Stanford University, Stanford, California 94305-2205*

Oscar A. Ruano

*Centro Nacional de Investigaciones Metalúrgicas, C.S.I.C., Av. de Gregorio del Amo 8, 28040 Madrid, Spain*

Jeff Wolfenstine

*Department of Mechanical and Aerospace Engineering, University of California at Irvine, Irvine, California 92717*

Oleg D. Sherby

*Department of Materials Science and Engineering, Stanford University, Stanford, California 94305-2205*

(Received 23 December 1991; accepted 30 March 1992)

A fine-grained ( $\bar{l} = 1.5 \mu\text{m}$ ) laminate containing 91.0 wt. % magnesium and 9.0 wt. % lithium was prepared by a foil metallurgy technique involving rolling and pressing at low homologous temperature (0.39–0.49  $T_m$ ). The processed material exhibits superplastic characteristics above 70 °C (0.40  $T_m$ ). The strain-rate-sensitivity exponent is about 0.5 and an elongation-to-failure of 450% was obtained at 100 °C (0.43  $T_m$ ). The activation energy for plastic flow in the superplastic region is 65 kJ/mole. This value of the activation energy is related to the expected activation energy for grain boundary diffusion.

## I. INTRODUCTION

The high stiffness and low density of magnesium-lithium alloys make them very attractive for weight-critical applications. In order to manufacture magnesium-lithium alloys into specific components with a minimum amount of machining and joining it is desirable to achieve superplasticity in these alloys. In general, superplasticity can be achieved in metallic alloys by developing a fine, equiaxed grain structure. A foil-metallurgy technique was previously used to prepare a fine-grained magnesium–9.0 wt. % lithium material with grain sizes,  $d$ , between 6 and 35  $\mu\text{m}$ .<sup>1,2</sup> The material exhibited superplastic behavior in the temperature range of 150 °C to 250 °C (0.49–0.61  $T_m$ , where  $T_m$  is the absolute melting temperature, 861 K). An important observation in these studies<sup>2</sup> was that the final grain size was a strong function of the amount of cold rolling prior to press-bonding; specifically, the greater the amount of cold rolling, the finer the grain size.

In order to minimize oxidation and surface reactions in magnesium-lithium materials during superplastic forming, it is necessary to achieve superplastic behavior at low homologous temperatures. It is the purpose of this paper, therefore, to assess the feasibility of a foil-metallurgy technique in preparing grain sizes finer than those previously studied ( $d < 6 \mu\text{m}$ ) and to investigate the superplastic behavior of the Mg–9Li material at low homologous temperatures (0.35–0.52  $T_m$ ).

## II. PROCESSING AND EXPERIMENTAL PROCEDURE

Magnesium–9.0 wt. % lithium (Mg–9Li) castings were supplied by the Naval Surface Weapons Center, Silver Spring, Maryland. This material is a binary, two-phase alloy, consisting of an hcp magnesium-rich phase,  $\alpha$ , and a bcc lithium-rich phase,  $\beta$ . The Mg–9Li alloy consists of approximately 30%  $\alpha$  and 70%  $\beta$  at room temperature. The microstructure of the as-cast alloy exhibits elongated grains of  $\alpha$ , with typical dimensions of 10  $\mu\text{m}$  by 150  $\mu\text{m}$ , embedded in a matrix of  $\beta$ .

The Mg–9Li material was received in the form of a cylindrical casting with a diameter of 38 mm and a length of 127 mm. The casting was cut into disks with lengths of 11.4 mm for subsequent processing. The first processing step for the Mg–9Li disks was to roll them at room temperature (0.35  $T_m$ ). The direction of rolling was parallel to the top and bottom surfaces of the disks. Rolling at room temperature was intermittently interrupted for 140 °C anneals of 30 min duration until a reduction of 48:1 was achieved. No recrystallization was observed after the 140 °C anneals. At this reduction, optical microscopy revealed a structure consisting of deformation bands parallel to the rolling direction.

After the reduction of 48:1, room temperature rolling was replaced by rolling with rolls heated to approximately 100 °C (0.43  $T_m$ ). Such warm rolling helped to eliminate edge cracking, and was done in

a continuous manner until a total reduction of 100:1 was achieved. After the one hundred-to-one reduction, 150 foils of dimensions  $51 \times 19 \times 0.11$  mm were cut. These rectangular foils were polished, stacked, and then press-bonded at a temperature of  $170^\circ\text{C}$  ( $0.53 T_m$ ). A total reduction of 500:1 was achieved after press-bonding. These pressed foils were further rolled at approximately  $100^\circ\text{C}$ , for a final total reduction of 1200:1.

Tensile strain-rate-change tests were conducted to determine the strain-rate-sensitivity exponent,  $m$ . Tensile samples with a gage length of 7.62 mm were machined from the laminated material. The testing direction was perpendicular to the pressing direction. A prestrain of about 15% engineering strain was introduced at the beginning of each test in order to form an isostructural condition; for the case of superplastic materials, an isostructural condition is represented by a constant, stable grain size. Strain-rate-change tests were conducted at temperatures ranging from  $25^\circ\text{C}$  to  $175^\circ\text{C}$  ( $0.35 \leq T/T_m \leq 0.52$ ) on an Instron machine equipped with a dual-elliptical furnace. The testing temperature was held constant to within  $\pm 2^\circ\text{C}$ . Constant cross-head speeds were used to conduct the strain-rate-change tests. Cross-head speeds were varied from  $8.5 \times 10^{-5}$  mm/s to as high as  $4.2 \times 10^{-2}$  mm/s. Each step in the strain-rate-change tests was carried out in such a way that a steady state flow stress was observed. Approximately 2% engineering strain was used per step. Where possible, each test series was immediately repeated upon reaching the highest speed. The second series of tests was used as a check for changes in microstructure, as evidenced by changes in the flow stress at a given true strain rate. In addition to the strain-rate-change tests, two elongation-to-failure tests were conducted in order to determine the tensile ductility of the material. These tests were also performed at constant cross-head speeds.

Microscopy was conducted throughout all processing steps as well as after tensile testing. The etchants used for evaluating the microstructure were (1) 10% hydrochloric acid in distilled water and (2) 1 ml nitric acid in 75 ml ethylene glycol.

### III. RESULTS

The optical micrograph in Fig. 1 shows the Mg–9Li laminate material after a reduction of 1200:1. A fine-grained recrystallized structure is clearly evident. Under scanning electron microscopy at magnifications of approximately  $5000\times$ ,  $\alpha$ - $\alpha$  and  $\alpha$ - $\beta$  grain boundaries were distinguishable, while  $\beta$ - $\beta$  grain boundaries were not distinguishable. The grain size of the processed material was measured on the basis of every distinguishable boundary, yielding a linear intercept

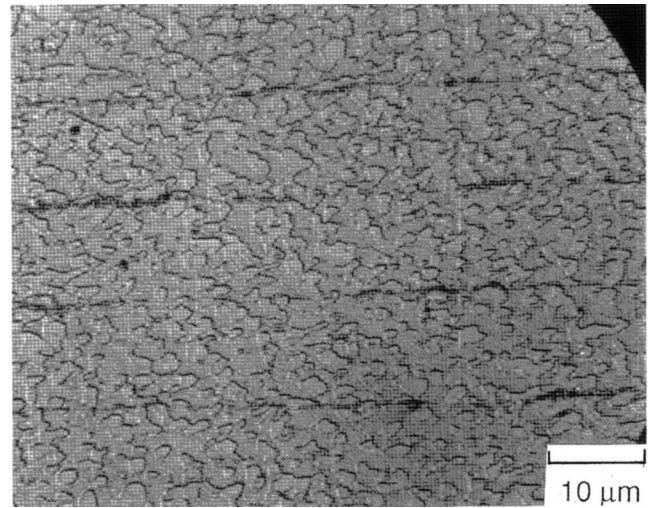


FIG. 1. Optical micrograph of the processed Mg–9Li laminate. The total reduction is 1200:1.

grain size of  $\bar{l} = 1.5 \mu\text{m}$  and a true grain size of  $d = 2.7 \mu\text{m}$  ( $d = 1.776\bar{l}$ ).<sup>3</sup> The photomicrograph in Fig. 1 reveals a foil thickness in the order of  $10 \mu\text{m}$ , and bonding was found to be good at foil interfaces. Previous studies have shown that the dark material at foil interfaces is not porosity, but  $\text{Li}_2\text{O}$  formed during processing.<sup>1</sup>

Figure 2 shows data from tensile strain-rate-change tests on a plot of the logarithm of the true strain rate versus the logarithm of flow stress. The open symbols represent the first strain-rate-change tests while the closed symbols represent the second strain-rate-change tests. On this plot the slope of the curves is equal to the stress exponent,  $n$  (where  $n = 1/m$ ). Slopes nearly equal to 2 were observed below a flow stress of 50 MPa. In this range, grain boundary sliding is believed to be the dominant deformation mechanism and superplastic behavior is expected.<sup>4</sup> At stresses above

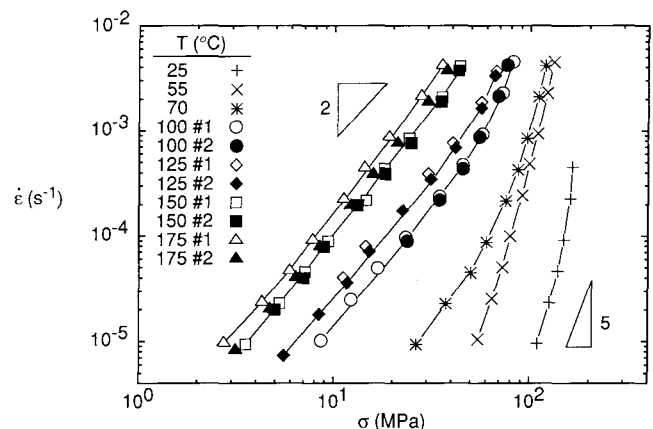


FIG. 2. Strain rate versus flow stress for the fine-grained Mg–9Li laminate material at several different temperatures.

50 MPa, a clear transition to much higher stress exponents can be seen ( $n \geq 5$ ), indicating the beginning of slip processes. No significant grain growth was observed at testing temperatures below 175 °C, and the grain size remained at  $d = 2.7 \mu\text{m}$ . This observation is in agreement with the flow stress remaining the same at a given strain rate for the two series of strain-rate-change tests. At 175 °C, however, some grain growth took place and a final grain size of  $d \approx 7 \mu\text{m}$  was observed; this grain growth contributed to an increase in flow stress in the strain-rate-change-test series, as seen in Fig. 2.

An elongation-to-failure test was conducted in the temperature and strain rate region where  $n \approx 2$ . The temperature was 100 °C and the initial strain rate was  $5.6 \times 10^{-4} \text{ s}^{-1}$ . An elongation to failure of 450% was achieved. This value is within the range of typical elongation-to-failure values exhibited by superplastic metallic alloys (300 to 1000%).<sup>4</sup>

A room temperature tensile test was conducted at an initial strain rate of  $1.1 \times 10^{-4} \text{ s}^{-1}$ , where slip processes are believed to control plastic deformation. Figure 3 shows the room temperature tension data on a plot of true stress versus engineering strain. An elongation to failure of 60% was observed. This is a remarkable elongation and cannot be attributed to strain hardening since the stress-strain curve exhibits a large strain softening region (Fig. 3). Furthermore, the high elongation is not likely explained by the strain-rate sensitivity since the strain-rate-sensitivity exponent is only about 0.1 ( $n = 10$ ). The sample exhibited uniform elongation with no necking until over 50% strain. The failure mechanism itself, however, was brittle-like with most of the fracture surface perpendicular to the tensile test direction. No shear lip was observed, unlike the case of most ductile metals. These unusual features in the Mg–9Li material are likely attributable to the presence of the two phases in an ultrafine-grained condition.

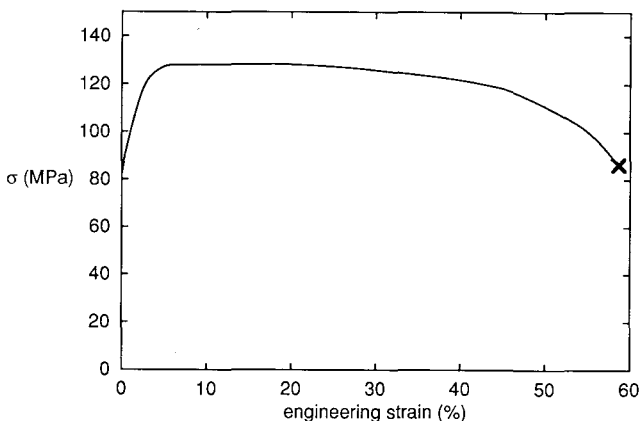


FIG. 3. Room temperature tensile test data for fine-grained ( $d = 2.7 \mu\text{m}$ ) Mg–9Li plotted as true stress versus engineering strain.

#### IV. DISCUSSION

The strain-rate-change test data (Fig. 2) were analyzed using the following constitutive equation:

$$\dot{\epsilon} = K \left( \frac{\mathbf{b}}{d} \right)^p \exp \left( - \frac{Q_c}{RT} \right) \left( \frac{\sigma}{E} \right)^n \quad (1)$$

where  $\dot{\epsilon}$  is the strain rate,  $K$  is a material constant,  $\mathbf{b}$  is the Burgers vector ( $\mathbf{b} = 3 \times 10^{-10} \text{ m}$ ),  $p$  is the grain size exponent,  $Q_c$  is the activation energy for creep,  $R$  is the gas constant,  $T$  is the absolute temperature,  $\sigma$  is the flow stress, and  $E$  is the dynamic Young's modulus.

An expression for  $Q_c$  can be obtained from Eq. (1) in terms of the strain rate and the temperature for a constant grain size, stress, and Young's modulus. This expression is of the form:

$$Q_c = -R \left. \frac{\partial(\ln \dot{\epsilon})}{\partial(1/T)} \right|_{d,E,\sigma} \quad (2)$$

From Eq. (2), a semilog plot of  $\dot{\epsilon}$  versus  $1/T$  yields  $Q_c/R$  as the negative of the slope of the data. Figure 4 is such a plot for Mg–9Li at two different flow stresses, for  $d = 2.7 \mu\text{m}$ , in the  $n \approx 2$  range. Young's modulus was assumed to be approximately constant since the temperature correction is very small at low homologous temperatures.<sup>5</sup> The average value for  $Q_c$  is 65 kJ/mole.

The superplastic behavior of the fine-grained Mg–9Li material ( $d = 2.7 \mu\text{m}$ ) can be compared with the previously obtained data for the intermediate grain size ( $d = 6$  to  $35 \mu\text{m}$ ) Mg–9Li material.<sup>1</sup> These earlier studies, based on samples tested at high homologous temperatures ( $0.49 \leq T/T_m \leq 0.61$ ), yielded a  $Q_c$  value equal to 104 kJ/mole in the  $n = 2$  region. This value is in good agreement with the predicted value for the activation energy of lattice diffusion,  $Q_L$ , in the  $\beta$  phase, which is 103 kJ/mole.<sup>1</sup> It was also shown that the grain size exponent,  $p$ , is equal to 2. It was postulated that superplastic flow in the intermediate grain size material

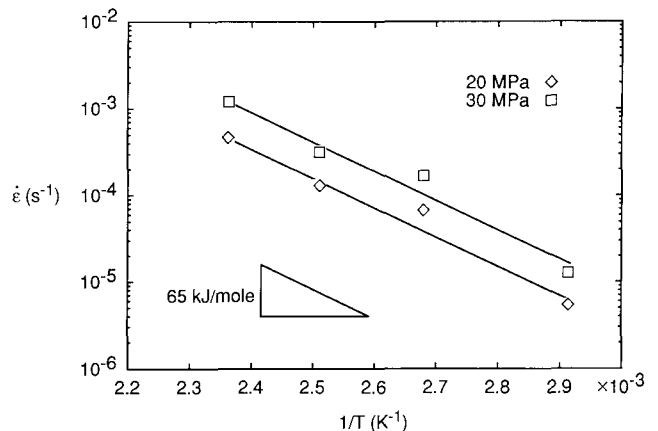


FIG. 4. Activation energy plot for Mg–9Li with  $d = 2.7 \mu\text{m}$  in the  $n = 2$  range.

was controlled by grain boundary sliding accommodated by slip controlled by lattice diffusion.<sup>1</sup>

The change in activation energy from 104 kJ/mole to 65 kJ/mole with decreasing temperature and grain size for the Mg–9Li material is in agreement with studies on other superplastic metallic alloys.<sup>4</sup> That is, it is generally observed that as the grain size and/or the temperature is decreased, the grain boundary sliding mechanism changes from lattice diffusion controlled to grain boundary diffusion controlled. The value of 65 kJ/mole obtained for the fine-grained Mg–9Li studied in this investigation cannot be compared with grain boundary diffusion data for this material, since no such data are available. Phenomenological relations, however, have been developed for determining the activation energy for grain boundary diffusion,  $Q_{gb}$ , in metallic materials at low homologous temperatures.<sup>6,7</sup> Hwang and Balluffi<sup>6</sup> predicted that  $Q_{gb}$  is equal to  $6.93 RT_m$  for  $0.22 < T/T_m < 0.42$  and  $9.35 RT_m$  for  $0.42 < T/T_m < 1.0$ . White<sup>7</sup> predicted that  $Q_{gb}$  is proportional to the lattice diffusion activation energy for a given crystal structure; the constant of proportionality is 0.67 for bcc metals and 0.59 for hcp metals. Thus, for the Mg–9Li materials,  $Q_{gb}$  predicted from Hwang and Balluffi is 50–67 kJ/mole, and  $Q_{gb}$  predicted from White for a bcc material is 70 kJ/mole. These values lead to the deduction that the activation energy observed for creep in the fine-grained Mg–9Li laminate is related to the activation energy for grain boundary diffusion.

The creep results for the fine-grained Mg–9Li alloy can be compared to the creep behavior of other superplastic metallic alloys that are also controlled by grain boundary diffusion. Extensive studies have shown,<sup>4,7,8</sup> based on data for twenty different superplastic alloys, that the following quantitative relation describes the creep rate for the case where superplastic flow is controlled by grain boundary diffusion:

$$\dot{\epsilon} = 10^8 \left( \frac{\sigma}{E} \right)^2 \frac{bD_{gb}}{\bar{l}^3} \quad (3)$$

where  $D_{gb}$  is the grain boundary diffusivity. Figure 5 is a plot of the logarithm of diffusion-and-grain-size-compensated strain rate versus the logarithm of modulus-compensated flow stress for the fine-grained ( $d = 2.6 \mu\text{m}$ ) Mg–9Li alloy. Young's modulus was calculated from Köster's data<sup>9</sup> for pure magnesium:  $E = 43.9 \text{ GPa}$  at  $70 \text{ }^\circ\text{C}$  and  $E = 41.8 \text{ GPa}$  at  $150 \text{ }^\circ\text{C}$ . The grain boundary diffusion coefficient was calculated from the relation:

$$D_{gb} = (D_0)_{gb} \exp\left(-\frac{Q_{gb}}{RT}\right) \quad (4)$$

where  $Q_{gb}$  was taken as equal to  $Q_c = 65 \text{ kJ/mole}$ , and  $(D_0)_{gb}$  was selected as  $10^{-4} \text{ m}^2/\text{s}$ , a value typically accepted for the pre-exponential constant.<sup>6,7</sup> The predicted

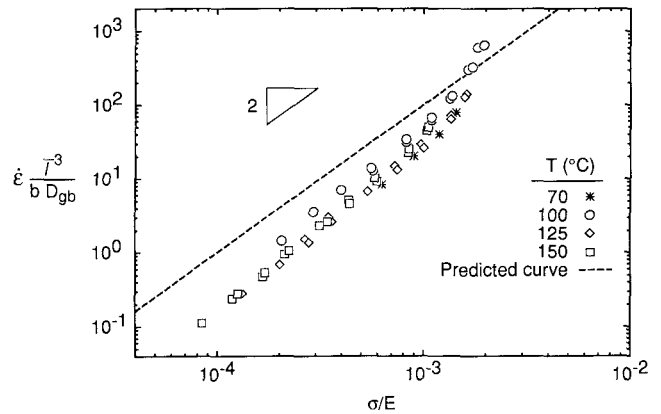


FIG. 5. Diffusion and grain-size-compensated strain rate as a function of modulus-compensated stress for the fine-grained Mg–9Li laminate material.

curve from Eq. (3) is shown in Fig. 5 by the dashed line. From Fig. 5 two important points are noted. First, all the data for the fine-grained Mg–9Li alloy superimpose on a common curve with a slope ( $n$ ) about equal to 2. Second, it is observed that the creep rate is within a factor of two to four of the predicted curve, indicating that superplastic flow of the fine-grained Mg–9Li at low homologous temperatures is similar to the behavior of other polycrystalline metals where superplastic flow is controlled by grain boundary diffusion.

## V. CONCLUSIONS

- (1) A fine-grained ( $\bar{l} = 1.5 \mu\text{m}$ ) Mg–9Li material has been prepared by cold-rolling and press-bonding foils at low homologous temperature ( $T \leq 0.42 T_m$ ).
- (2) At temperatures from  $70 \text{ }^\circ\text{C}$  to  $150 \text{ }^\circ\text{C}$  and flow stresses below 50 MPa, Mg–9Li with  $\bar{l} = 1.5 \mu\text{m}$  exhibits superplastic behavior with a stress exponent of approximately 2 and a creep activation energy of 65 kJ/mole.

(3) A tensile elongation of 450% was obtained at a low homologous temperature of  $0.43 T_m$  ( $100 \text{ }^\circ\text{C}$ ). Even at room temperature ( $0.35 T_m$ ) a high elongation of 60% was achieved.

(4) At the fine grain size ( $\bar{l} = 1.5 \mu\text{m}$ ) and low homologous temperatures ( $T \leq 0.49 T_m$ ) used, it is postulated that superplastic flow in the Mg–9Li alloy is controlled by grain boundary sliding accommodated by slip controlled by grain boundary diffusion.

## ACKNOWLEDGMENTS

The United States Office of Naval Research provided financial support for this program under Contract No. N-00014-91-J-1197. The authors gratefully acknowledge technical advice and assistance from Dr. George Yoder, Materials Branch, O.N.R., and Mr. A. P. Divecha, Naval Surface Weapons Center, Silver Spring, Maryland.

Jeff Wolfenstine would like to thank the University of California at Irvine for a Faculty Research Grant 91/92-02FRG.

## REFERENCES

1. P. Metenier, G. González-Doncel, O. A. Ruano, J. Wolfenstine, and O. D. Sherby, *Mater. Sci. Engng.* **A125**, 195 (1990).
2. J. Wolfenstine, G. González-Doncel, and O. D. Sherby, "Processing and Elevated Temperature Properties of Mg–9Li Laminates," *Metal and Ceramic Matrix Composites: Processing, Modeling and Mechanical Behavior*, edited by R. B. Bhagat, A. H. Clauer, P. Kumar, and A. M. Ritter (The Minerals, Metals and Materials Society, Warrendale, PA, 1990), pp. 263–270.
3. A. Ball and M. M. Hutchinson, *Met. Sci. J.* **3**, 1 (1969).
4. O. D. Sherby, R. D. Caligiuri, E. S. Kayali, and R. A. White, "Fundamentals of Superplasticity and its Applications," *Advances in Metal Processing*, edited by J. J. Burke, Robert Mehrabian, and Volker Weiss (Plenum Press, New York, 1981), pp. 133–170.
5. C. R. Barrett, A. J. Ardell, and O. D. Sherby, *Trans. AIME* **230**, 200 (1964).
6. J. C. M. Hwang and R. W. Balluffi, *Scripta Metall.* **12**, 709 (1978).
7. R. A. White, Ph.D. Dissertation, Stanford University (1978), Stanford, CA 94305.
8. O. D. Sherby and J. Wadsworth, "Development and Characterization of Fine-Grain Superplastic Materials," *Deformation, Processing and Structure*, edited by G. Krauss (ASM, Metals Park, OH, 1984), pp. 355–389.
9. W. Köster, *Z. Metallkd.* **39**, 1 (1948).